Materials Physics and Mechanics 47 (2021) 266-284 Received: October 2, 2020

INFLUENCE OF THE SIZE OF TURMERIC MICROPARTICLES REINFORCING AGENT ON MECHANICAL AND BIODEGRADATION PROPERTIES OF CORNSTARCH-BASED BIOPLASTIC MATERIAL: CURRENT STUDIES, EXPERIMENTAL RESULTS, AND PROPOSAL MATERIAL CRACK PHENOMENA DURING MECHANICAL TESTING

A.B.D. Nandiyanto[1*], F. Triawan[2], M. Fiandini[1], I.O. Suryani[2], G.K. Sunnardianto[3]

[1]Departemen Kimia, Universitas Pendidikan Indonesia, Jl. Dr. Setiabudhi No. 229, Bandung, Indonesia

[2]Department of Mechanical Engineering, Faculty of Engineering and Technology, Sampoerna University, Jl. Raya Pasar Minggu No. 16, Jakarta, Indonesia

[3]Research Center for Physics, Indonesian Institute of Sciences (LIPI), Kawasan Puspiptek Serpong, Tangerang Selatan, 15314, Indonesia

*e-mail: nandiyanto@upi.edu

Abstract. The purpose of this study was to investigate the effect of sizes of turmeric microparticles (as a reinforcing agent) on the mechanical and biodegradation properties of cornstarch-based bioplastic material. The following fabrication procedures were performed: (1) diluting cornstarch in water; (2) making homogeneous mixture of cornstarch, glycerol and acetic acid by heating at less than 100ºC, (3) additional turmeric with a specific size (i.e. 250, 125, 100, 74 μm); (4) molding process; and (5) drying process to obtain solid bioplastic materials. This study shows the importance of reinforcing agent size for improving the mechanical properties of bioplastic materials. The smaller turmeric size brings better mechanical properties than the larger turmeric size that has more void space. To support the analysis, the present study also was completed with a literature review regarding bioplastic production and proposal bioplastics material crack phenomena during mechanical testing.
Keywords: bioplastics, cornstarch, particle size, mechanical properties, turmeric

1. Introduction

The synthesis of bioplastics based on biodegradable materials has been attracted tremendous attention. One of the attractive materials is starch-based bioplastics. However, starch-based bioplastics have disadvantages such as poor performance, hydrophilicity, and resistance to moisture [1].

To solve problems regarding the limitation of starch-based bioplastics, several strategies have been implemented. Bioplastics were usually formed from a combination of several materials, one of which acts as the main material and the other as reinforcing agents. In addition to the additional reinforcing agents, several parameters must be considered [2,3], including size [4-6], composition [7-9], shape [10], and surface structure [11,12].

Based on our previous studies [13,14] regarding the use of micrometer-sized starch particles and their composition impacts on the bioplastic performance, the present study aims

http://dx.doi.org/10.18149/MPM.4722021_9

to examine the effect of turmeric microparticles' size on the mechanical and biodegradation properties of cornstarch-based bioplastic material. Turmeric was selected since it is enriched with natural antimicrobial, accessible material at relatively low cost, and having high biodegradability. Different from other studies that mostly focused on composition, the present study considered the use of micrometer-sized raw material. While other reports did not concern about the particle size, the present study focused on the effect of particle size of raw materials, which this study brings excellent insight for the development of bioplastic material. To support the analysis, the present study also was completed with a literature review regarding bioplastic production and proposal bioplastics material crack phenomena during mechanical testing.

2. Materials and Method

Preparation of Cornstarch-based Bioplastic Material. This study used micron-sized cornstarch particles (purchased from PT Egafood, Jakarta, Indonesia), turmeric (*Curcuma Longa*; collected from Bandung, Indonesia), acetic acid (25%; purchased from Sakura Medical Stores, Bandung, Indonesia), glycerol (95%; purchased from Sakura Medical Stores, Bandung, Indonesia), and distilled water (purchased from Sakura Medical Stores, Bandung, Indonesia). The experimental procedure is explained in Fig. 1.

Turmeric was washed, sliced into small pieces, and dried to remove the existence of water using an electrical furnace under atmospheric conditions. Dried turmeric was ground and mashed using a saw-milling process with a rotating speed of 18,000 rpm to obtain homogenous milling. Detailed information about the saw-milling process is explained in previous literature [15]. To obtain a specific size the milled turmeric was put into sieve test measurement with (PT Rumah Publication Indonesia, Indonesia with various holes of 2000, 1000, 530, 250, 125, 99, 74, 58, and 48 μm).

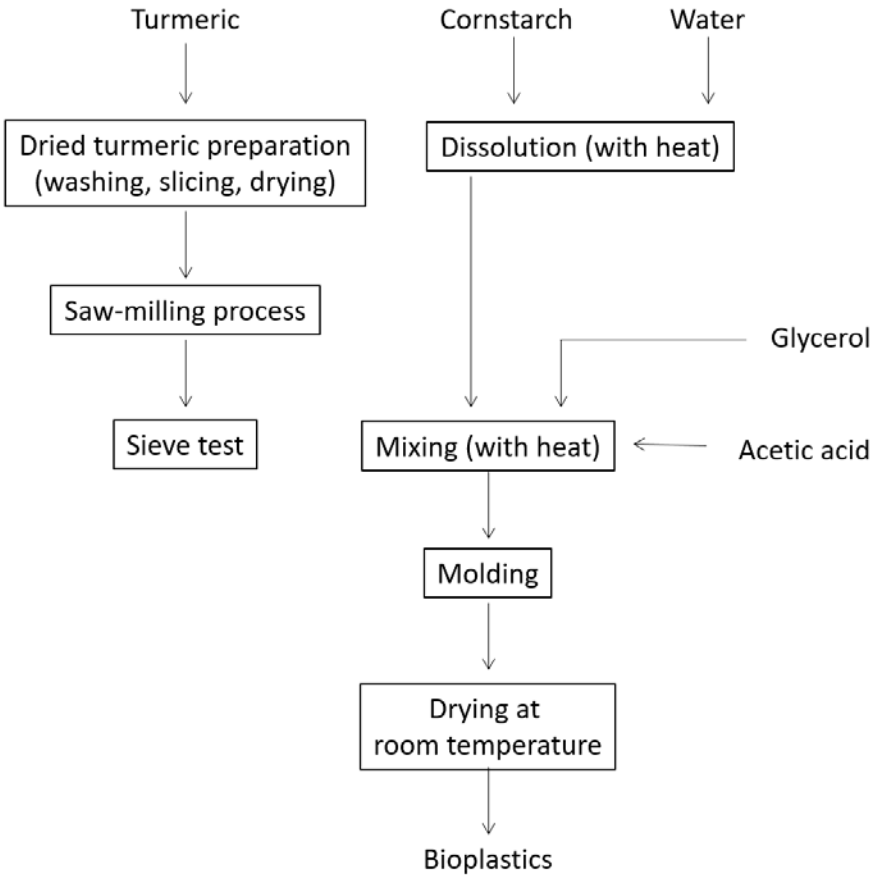

Fig. 1. Experimental procedure for the preparation of bioplastic

In the experimental procedure, to produce bioplastics, the following steps were carried out. The starch solution was prepared by dissolving cornstarch in distilled water and heating the mixture. Then, we added 95% of glycerol, 25% of acetic acid, and turmeric powder with various sizes of 250, 125, 100, and 74 μm, and the mixture was stirred until it gets homogeneous. At the same time with the gelatinization and manual mixing process, the mixture was heated at 60°C for 30 minutes using an electrical heater to obtain a viscous product. The viscous product was molded and dried at room temperature for more than 24 hours until it formed a solid yellow film.

Physicochemical properties. The morphology of the prepared samples was analyzed using a Digital Microscope (BXAW-AX-BC, China). To support the analysis, we conducted characterizations using a Fourier Transform infrared (FTIR-4600, Jasco Corp., Japan).

Mechanical properties. The observation of the bioplastic turmeric mechanical properties was observed using a compression test. The compression test was performed using 313 Family test machines at a scan rate of 1 mm/s at a temperature of 24°C and humidity of 10%, respectively. The compression test preparation was done by measuring the dimension of the sample using Vernier caliper and coat the compression plate using the lubricant. In this case, the lubricant is Vaseline that aims to reduce the friction effect.

Table 1 shows the mesh variation of the sample and its corresponding dimension. Data collected from compression tests such as Load vs Displacement, Stress vs Strain, and Young's modulus were evaluated for each sample to analyze its mechanical properties.

Table 1. Sample dimension

Sample, mesh	Particle size, μm	Dimension (length × width × thickness), cm
60	250	2.00 × 2.00 × 0.50
120	125	2.00 × 2.00 × 0.70
150	100	2.00 × 1.70 × 0.70
200	74	2.00 × 2.00 × 0.50

The following formula can be used to process the raw data from the compression test for further analysis:

(1) *Ultimate compression strength* (MPa) is defined as the maximum force that can be held in the sample when being compressed before the material is broken. The ultimate compression strength can be calculated by dividing maximum stress (F_M; N) with the cross-section area of the specimen (A; mm^2) as shown in Eq. (1).

$$\text{Compression strength} = \frac{F_M}{A}. \quad (1)$$

(2) *Young's modulus* (MPa) is a mechanical property that measures the stiffness of elastic deformation of specimens under a given load. Young's modulus can be obtained from the slope of the stress-strain since defines the relationship between stress (σ) and strain (ε) of material deformation in the linear elasticity regime. Young's modulus can be determined using Eq. (2).

$$\text{Young's Modulus} = \frac{\sigma_2 - \sigma_1}{\varepsilon_2 - \varepsilon_1}, \quad (2)$$

where ε_1 and ε_2 are the conditions of relative elongation and σ_1 and σ_2 are the stress that occurs at ε_1 and ε_2, respectively. The method of observing the slope-strain of the sample for defining Young's modulus is adopted since the slope of the sample can be directly observed as a function of the material deformation (strain)[16].

Biodegradability. The biodegradability tests were conducted by slicing the prepared bioplastics with sizes of about 5 × 5 × 5 mm and then immersing them into ultrapure water. The weight losses of the sample were measured at the interval time of two days. In line with this test, during the immersing process, it was also visually observed the change of color. Detailed information about the biodegradability test is explained in our previous report[13].

3. Results and Discussion

Current reports on the preparation of bioplastics. To form a better bioplastic performance, the bioplastic raw materials were usually a combination of several materials, one of which acts as the main material and the other as reinforcing agents. The most recent reports on the synthesis of bioplastic materials with reinforcing agents are presented in Table 2.

Production of cornstarch-based bioplastics with varying turmeric microparticles. The production of cornstarch-based bioplastics with the addition of turmeric microparticles size variations is shown in Fig. 2. Visually, the bioplastic is yellow with the addition of turmeric to the cornstarch-based bioplastic. Figures 2(a-d) is a bioplastic appearance with variations in the size of turmeric: (a) 250, (b) 125, (c) 100, and (d) 74 μm. The large particle size of turmeric causes the bioplastic to crack more easily than the smaller particle size of turmeric.

The microscope analysis of bioplastic with the addition of turmeric size variations is shown in Fig. 2(e-j). Figures 2(e) and (f) are materials for the fabrication of bioplastics, namely micron-sized corn and variations size of turmeric powder, respectively. Micrometer-sized cornstarch particles were white crystals, solid, and dense. Turmeric powder has a yellow color, heterogeneous surface, and agglomerated. Figures 2(g-h) are the bioplastic surface appearance with variations in the size of turmeric of 250, 125, 100, and 74 μm, respectively. The bioplastic surface with the smallest turmeric size has a more homogeneous surface and is less brittle compared to the large turmeric size because of the size of the starch, which is almost the same as the size of turmeric that has a rigid structure. Figure 2(k) is the appearance of the bioplastic after being immersed for 6 days in water. The color of the bioplastic starts to change from yellow to brownish-yellow. It can be observed that after 6 days of immersion, cracks were found due to the swelling phenomenon. Figure 2(l) is the appearance of the bioplastic after being immersed for 4 weeks. The bioplastic surface with immersion for 4 weeks experienced a bad brittle phenomenon and a black fungus appears on the bioplastic surface.

Figure 3 shows the proposal formation mechanism of bioplastics prepared from the combination of cornstarch and turmeric with glycerol. The mechanism has used the assumption of two-particle interaction (i.e. Particle A and B) and they attach each other with glycerol (red molecule). Particles A and B have chemical structures of CR1 and CR2, respectively. CR1 and CR2 can be from starch (shown as green molecule) or turmeric (presented as blue molecule). In short, the polymerization was started from the interaction between Particle A and glycerol (see route R1). Then, additional heat treatment and catalyst (such as acetic acid), the interaction continues to the formation of glycerol-Particle A bonding (by releasing OH group). When there are other movements of Particle B (see route R2) to the surface of the glycerol-Particle A component (see route R3), another polymerization happens. This makes the final component contained a packed balls-like structure[13].

Table 2. Current reports on the synthesis of bioplastic with an additional reinforcing agent

Type of carbohydrate	Reinforcing agent	Raw material	Results	Ref.
Cassava starch	Zinc oxide/clay	Cassava starch, glycerol, distilled water, zinc oxide/organoclay	Additional zinc oxide/clay improve mechanical properties. The best ratio with the addition of 0.3:0.7 of zinc oxide/clay has a tensile strength of 20.87 MPa	[17]
	Oil palm	Cassava starch, oil palm, glycerol, and distilled water	Additional oil palm has not increased mechanical properties. However, it accelerated biodegradation	[18]
	Chitosan and Kraft fiber	Cassava starch, distilled water, Kraft fiber, chitosan, acetic acid, and glycerol	The best bioplastic with the addition of 30% of Kraft fiber and 4% of chitosan had properties similar to polystyrene foam	[19]
	Pumpkin residues and oregano essential oil	Cassava starch, pumpkin residues (skin), oregano essential oil, glycerol, 2,2-diphenyl-1-picrylhydrazyl radical (DPPH), thiobarbituric acid (TBA), trichloroacetic acid (TCA), butyl hydroxyl toluene (BHT), 1,1,3,3-tetraethoxypropane (TEP)	Compared with pumpkin residues (skin), bioplastic with oregano essential oil increased antimicrobial activity	[20]
	Cornstarch	Cassava starch, cornstarch, glycerol, distilled water	Starch-based bioplastics (40 g/kg) had mechanical properties comparable to LDPE-based films	[21]
	Polycaprolactone (PLC)	Cassava starch, Polycaprolactone (PLC), glycerol, and ethanol (99.8% v/v absolute ethyl alcohol	Bioplastic made from a mixture of PCL/cassava starch does not improve the mechanical properties	[22]

Table 2 (continue). Current reports on the synthesis of bioplastic materials

Type of carbohydrate	Reinforcing agent	Raw material	Results	Ref.
Cornstarch	Taro starch nanoparticles (TSNPs)	Cornstarch, taro starch,	Bioplastic with the addition of taro starch increased tensile strength from 1.11 to 2.87 MPa. However, increased concentration of taro starch decreases water vapor permeability (WVP) of bioplastic	[23]
	Palm fibers	Cornstarch, palm fibers, NaOH, acetic acid, glycerin, and distilled water	The additions of the reinforcement (palm fibers) improve the tensile strength, biodegradation, Young's modulus, and water uptake.	[24]
	Cornhusk fiber	Cornstarch, corn husk fiber, fructose, and distilled water	Bioplastics with the addition of husk fibers improve mechanical properties and thermal stability. However, it decreases biodegradation	[25]
	Barley straw (*Hordeum vulgare L.*)	Cornstarch (CS), glycerol, distilled water, and Barley straw (*Hordeum vulgare L.*)	Bioplastic with the addition of 15% of barley straw increased tensile strength, Young's modulus, and thermal stability	[26]
	Sisal fibers	Cornstarch, sisal fiber, and glycerol	Sisal fibers increase tensile strength and Young's modulus. It also improved chemical modification in matrix	[27]
Sugar palm starch	Sugar palms Nano fibrillated cellulose (SPNFCs)	Sugar palms fiber, sugar palm starch, Sodium hydroxide, sodium chlorite (80% purity), acetic acid, sorbitol, and glycerol	It increased water barrier properties sugar palm-based bioplastic	[28]
Jack fruit seed starch	Banana fruit skin powder (BSP)	Jack fruit starch, banana fruit skin powder, distilled water, and glycerol	The best bioplastic with the addition of 1% of banana skin powder had maximum tensile strength of 10.90 MPa and good biodegradability	[29]

Table 2 (continue). Current reports on the synthesis of bioplastic materials

Type of carbohydrate	Reinforcing agent	Raw material	Results	Ref.
Potato starch	Corn fibers and poly (vinyl alcohol) (PVA)	Potato starch, corn fibers, distilled water, and glycerol	The addition of corn fiber decreases mechanical properties and improved water resistance.	[30]
	Wood fiber	Potato starch, wood fiber, guar gum, and magnesium stearate	40% of wood fiber has the highest tensile strength of 128 MPa and Young's modulus of 3200 MPa	[31]
	Titanium oxide nanoparticles (TiO_2 NPs)	Potato starch, titanium oxide nanoparticles (TiO_2-NPs), distilled water, and glycerol	The addition of TiO_2-NPs at low concentrations improved the mechanical properties and moisture barrier of the bioplastic.	[32]
Pea starch	Waxy maize starch nanocrystals	Pea starch (about 40% amylose), Waxy maize starch (98% amylopectin), glycerol, sulfuric acid, potassium carbonate.	Bioplastics with the addition of waxy maize nanocrystals increase tensile strength. The highest tensile strength values contain 5% of waxy maize nanocrystals	[33]
Wheat gluten	Coconut fiber	Wheat gluten, (3-triethoxysilylpropyl)-tbutylcarbamate (carbamate silane) sodium hydroxide, and coconut fiber	Bioplastics with the addition of coconut fiber increase the tensile strength by 80%	[34]
	Flax fiber	Wheat gluten powder, glycerol, ethanol, and flax fiber	19% of flax fiber improved the quality crack resistance and stress maximum from 2 to 29 MPa. The bioplastic surface is homogeneous	[35]
	Lignin nanoparticles (LNP)	Wheat gluten, lignin nanoparticles, distilled water, glycerol, and hydrochloric acid	Bioplastic with the addition of LNP increased mechanical properties, thermal stability, and water sensitivity. However, the transparency of bioplastic decreases	[36]

Table 2 (continue). Current reports on the synthesis of bioplastic materials

Tamarin seed	Banana fiber	Tamarin seed, banana fiber, distilled water, and glycerol	The temperature condition of tamarind seeds 130°C has the highest tensile strength of 3.97 MPa	[37]
Banana peel	Cornstarch	Banana peel, cornstarch, hydrochloric acid, glycerol, and sodium hydroxide	4% of cornstarch has the highest tensile strength of 34.72 N/m^2	[38]
	Zinc oxide (ZnO)	Banana peel, glycerol, chitosan flakes, NaOH, glacial acetic acid, distilled water, and zinc oxide	Bioplastic composition with 4-30% of chitosan, starch, glycerol, 5% of ZnO shows the bioplastic with the best microbial activity	[39]

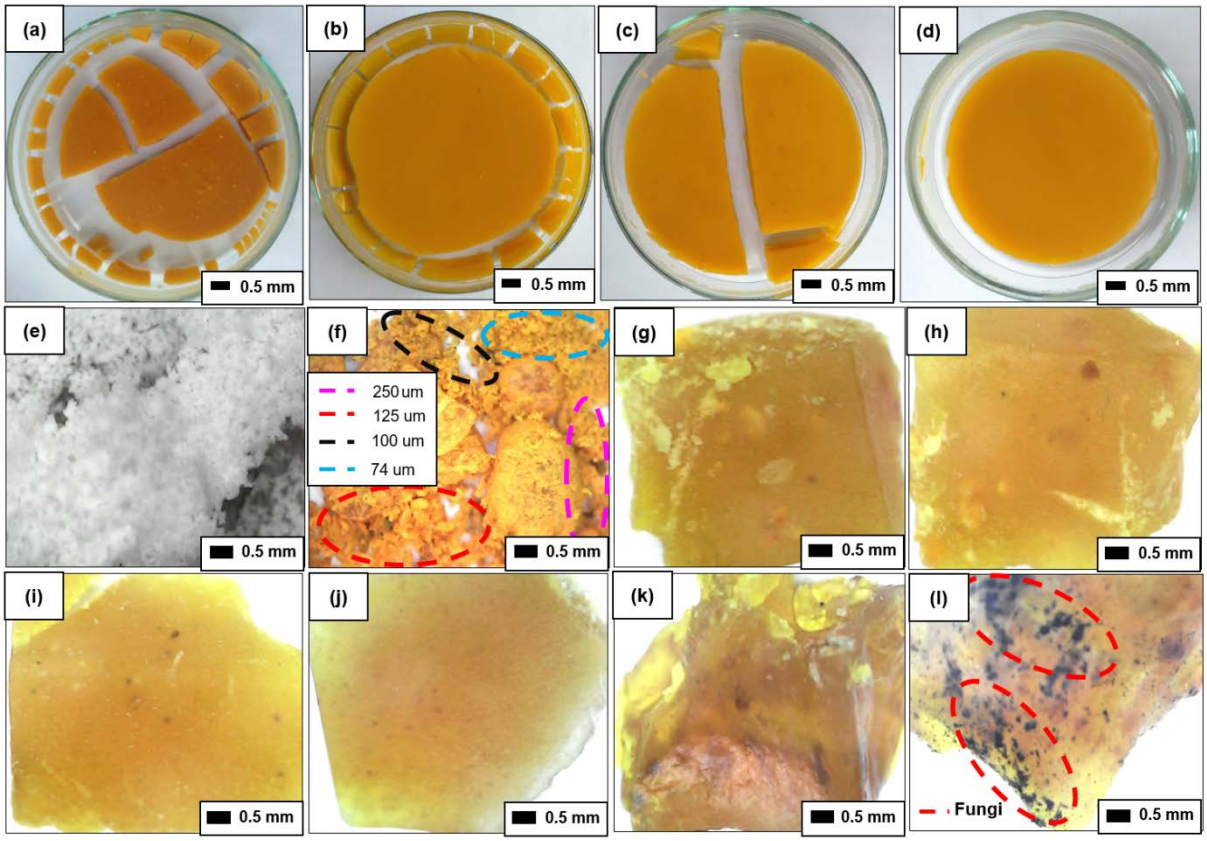

Fig. 2. Photograph image of cornstarch-based bioplastics with the addition various size turmeric (a) 250, (b) 125, (c) 100 and (d) 74 μm. Microscope images of (e) micro-sized cornstarch, (f) turmeric powder, (g-j) bioplastic prepared using turmeric with sizes of 250, 125, 100, 74 μm, respectively, (k) bioplastics after 6 days immersed in water and (l) fungi bioplastic after 4 weeks immersed in water

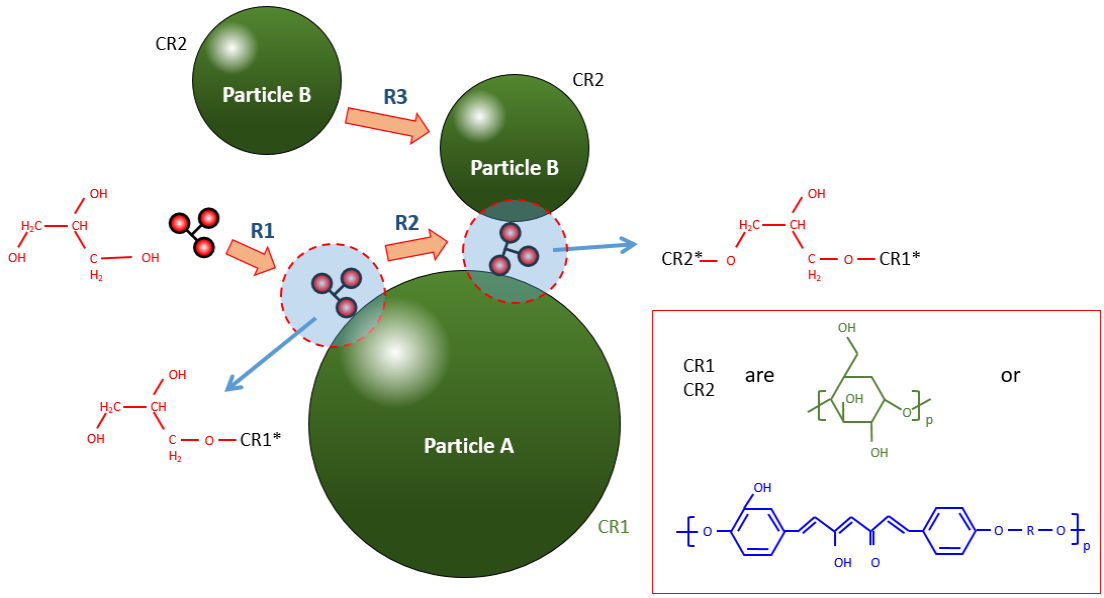

Fig. 3. Proposal reactions during the polymerization in the formation of bioplastic. Particles A and B have the chemical structure of CR1 and CR2 respectively. CR1 and CR2 can be from starch or turmeric

Biodegradability of cornstarch-based bioplastics with varying turmeric microparticles. To confirm the phenomenon during the immersion process as shown in Figs. 2(k) and (l), Fig. 4 shows the results of the FTIR analysis results of as-prepared bioplastics, bioplastics immersed for 2 weeks in water, and the surface of the bioplastic samples immersed for 4 weeks. The as-prepared bioplastic content results were identified at wavelengths of 1014, 1723, and 3300 cm^{-1} [40]. The comparison of the FTIR peaks for bioplastics before and after 2-week immersion in water confirms that the biodegradability in water was only the dilution of the outer component on the bioplastics. The reaction between water and bioplastics involves a dilution process and did not interfere with complicated reactions.

We also found that immersion for 4 weeks caused the appearance of fungi on the bioplastic surface. The bioplastic surface analysis shows that the fungus degrades the bioplastics, converting the bioplastic chemical structure to the fungal structure (see the green dashed area in Fig. 4) [41].

To confirm the weight losses during the immersion process, we analyzed the mass of bioplastic as a function of the day (see Table 3). Table 3 shows the results of bioplastic weight loss carried out for a week. The results showed that bioplastics' weight decreased for 4 days of immersion in water. The possible weight loss during 2-week immersion is because the bioplastics' outer surfaces were diluted in water, confirmed by the identical FTIR patterns. This result is different for 4-week immersion bioplastic, in which the mass loss was followed by the appearance of fungus (see Fig. 2 (l)) and fungus chemical structure (see Fig. 3). The present bioplastics were made from cornstarch, making microorganisms more easily break the polymer chain inside the bioplastics themselves [41]. In addition, compared to the bioplastic prepared from cornstarch only [13], the decomposition of the present bioplastic is slower. The existence of turmeric deters the growth of microorganisms since turmeric has an antiseptic effect.

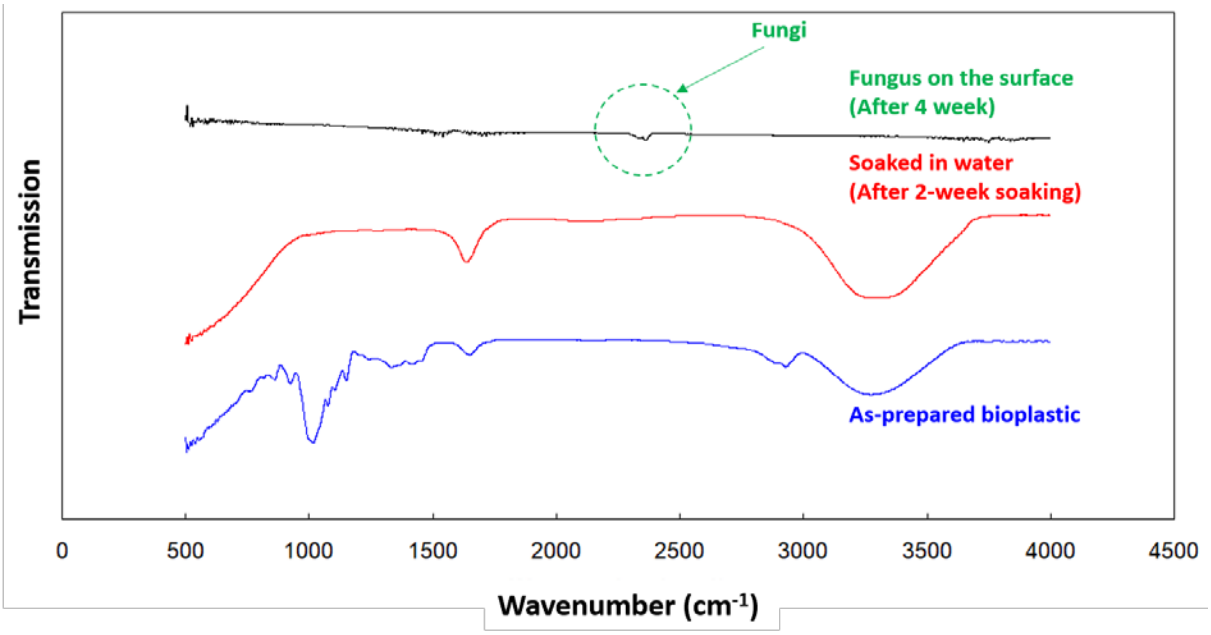

Fig. 4. FTIR analysis results of as-prepared bioplastic, 2-week immersed bioplastic in water, and fungus on the 4-week immerged sample

Mechanical properties of cornstarch-based bioplastics with varying turmeric microparticles. The mechanical properties of samples were determined by applying load gradually to the samples and measuring their deformation [42]. The load and deformation data is then used to obtain the stress and strain curve [43]. The stress-strain curve of bioplastic samples with variation of micrometer size is presented in Fig. 5. Based on the stress-strain curve, the ultimate strength is determined from the first peak of the stress-strain curve (see Fig. 6). Table 4 summarizes the ultimate strength of all samples. The curve shows a random trend where the highest ultimate strength achieved by the sample of 74 μm and the lowest ultimate strength obtained from sample of 125 μm while sample of 250 μm is in between.

The ultimate strength values of samples prepared using turmeric particles size of 74, 100, and 125 μm are 2563, 1618, and 1164 kPa respectively (Table 4). It shows the decreasing value of ultimate strength with the increasing particle size of the sample. Smaller particles have a higher total surface area of the filler particles, allowing more efficient stress transfer mechanisms and resulting in the higher ultimate strength of the sample [44]. Smaller particles also affect the adhesive factor that increases intermolecular bonding, hence resulting in higher material strength. However, the larger particles (sample of 250 μm) did not show the same characteristics. This could be caused by the microstructural mechanism, thus further observation on sample morphology needs to be performed to observe this phenomenon.

Table 3. Weight loss bioplastics with addition of size turmeric during immersion process

Size (um)	Days	Initial Dimension, cm^2	Initial mass, g	Mass after Immersion, g	Mass loss, wt%	Decay dimension, g/cm^2
250	1	1.084	0.133	0.080	40	0.050
	2	1.161	0.113	0.053	53	0.051
	4	1.216	0.143	0.063	56	0.067
	6	1.128	0.100	0.040	60	0.055
	8	0.972	0.137	0.047	66	0.102
	10	1.115	0.143	0.043	70	0.095
	14	1.117	0.140	0.037	74	0.104
125	1	1.090	0.123	0.077	38	0.043
	2	1.249	0.117	0.057	51	0.047
	4	1.165	0.190	0.083	56	0.092
	6	1.262	0.137	0.043	68	0.074
	8	1.268	0.137	0.040	71	0.077
	10	1.220	0.147	0.037	75	0.092
	14	1.242	0.133	0.030	77	0.084
100	1	1.013	0.127	0.073	43	0.053
	2	1.127	0.110	0.063	45	0.043
	4	1.044	0.130	0.050	62	0.077
	6	0.894	0.117	0.037	68	0.094
	8	1.188	0.137	0.037	73	0.090
	10	1.290	0.143	0.033	77	0.087
	14	1.274	0.143	0.030	79	0.093
74	1	0.895	0.150	0.110	28	0.045
	2	1.080	0.133	0.053	60	0.075
	4	0.960	0.137	0.047	66	0.096
	6	1.124	0.147	0.043	70	0.092
	8	1.020	0.133	0.033	75	0.099
	10	0.870	0.140	0.027	81	0.135
	14	1.010	0.133	0.020	85	0.114

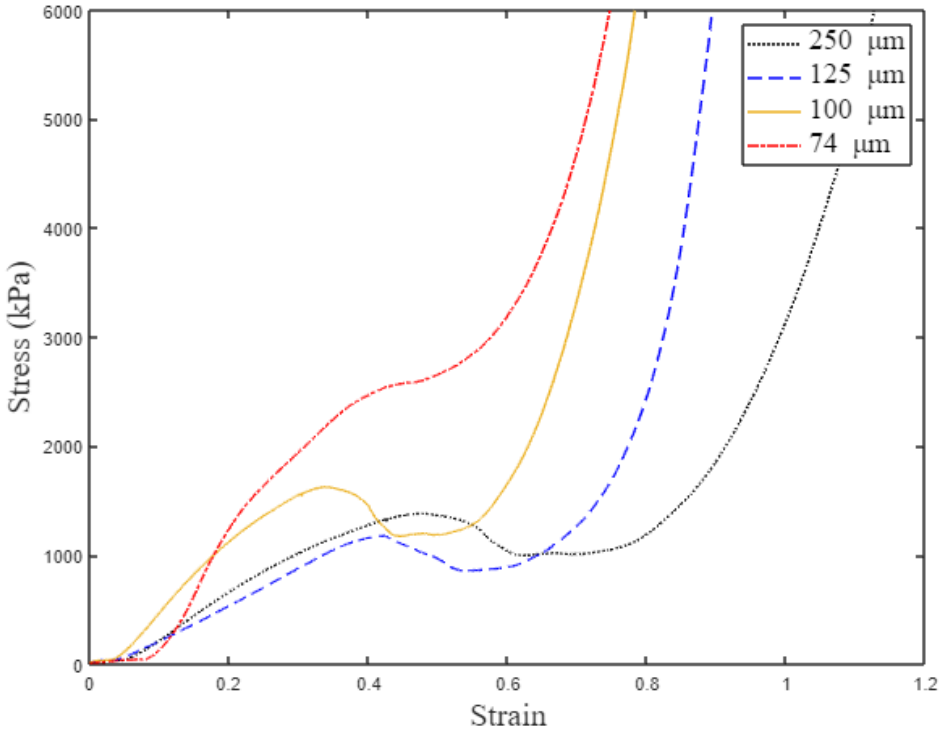

Fig. 5. Stress vs Strain of bioplastic samples

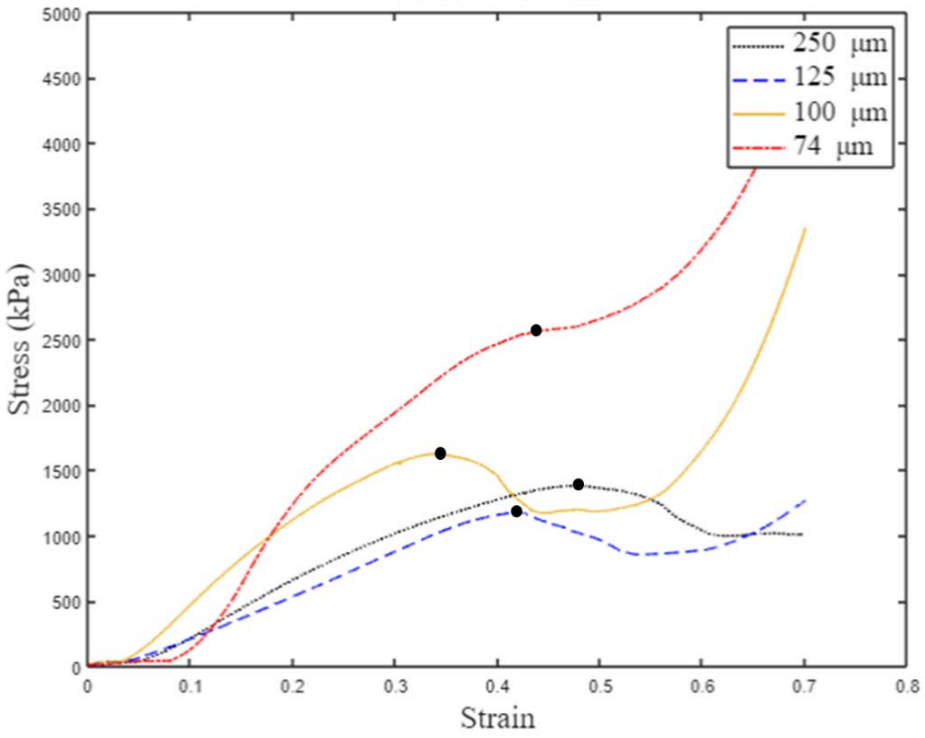

Fig. 6. Stress vs Strain of bioplastic samples limited at strain of 0.70 and stress of 4500 kPa

Table 4. The ultimate strength of bioplastic samples

Sample, μm	Ultimate strength, kPa
250	1379
125	1164
100	1618
74	2563

Variation of particle size affecting the Young's modulus (stiffness) of the sample. As the particle size increases, the stiffness of the sample tends to decrease as shown in Fig. 7. The highest slope of stress-strain curve shown in Fig. 7 indicates the Young's modulus value of each sample, in which the sample with particle sizes of 74, 100, and 125 μm are 14780, 7724, and 2626 kPa, respectively (Table 5). The addition of small microparticles to the polymatrix result in higher Young's modulus as they have higher intermolecular bonding in the larger area, making the material difficult to deform as a load is applied. Different trends for the sample with particle sizes of 250 μm that has Young's modulus of 5116 kPa need to be observed in terms of its microstructure, as previously reported that microstructure (due to particle size distribution) affects the material stiffness.

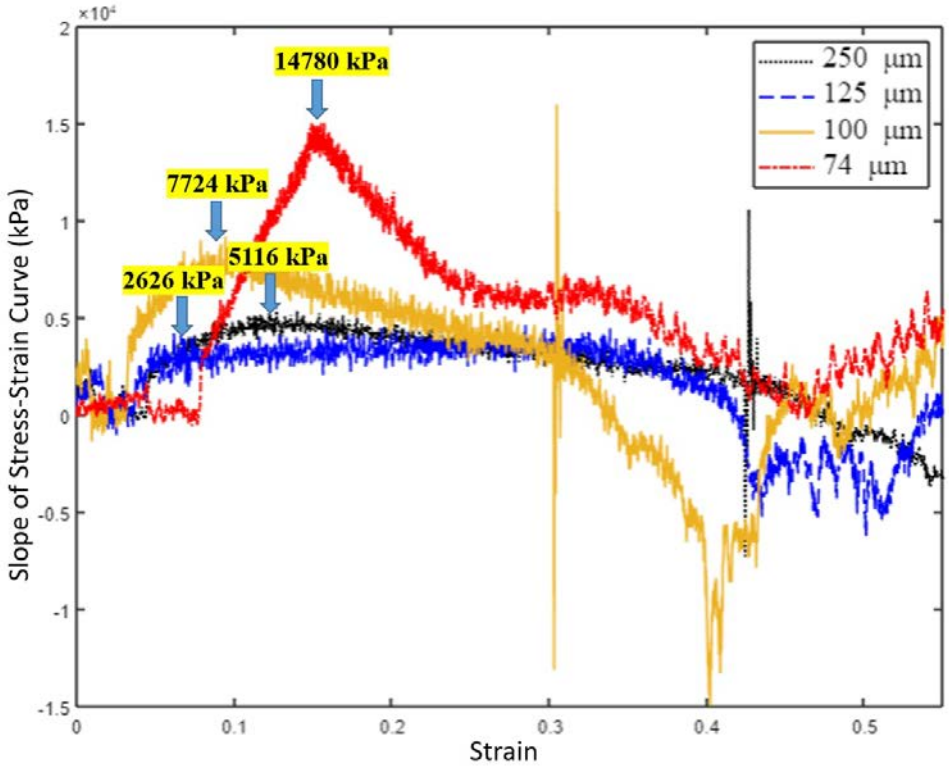

Fig. 7. Young's modulus vs Strain of bioplastic samples

Table 5. The Young's moduli of bioplastic samples

Sample, μm	Young's modulus, kPa
250	5116
125	2626
100	7724
74	14780

Proposal cornstarch-based bioplastics crack. To get deeper insights into the bonds, area having a minimum and maximum stress concentration, and the bond-breaking initiation, an illustrative model is qualitatively shown in Fig. 8. The figure shows a particle stress distribution evolution, a bond breaking, crack nucleation, and growth scenario of the system during the applied compression test. The concept was derived from the existence of particle-particle interaction based on Fig. 3. The polymerization happens on the surface of the particle, and there is no change in the chemical composition inside the particle.

Figure 8(a) shows stress distribution before bond breaking. Prior to the applied stress, the particle arrangement was in the perfect lattice site. At the initial stage of loading, the particle position of chains started to shift from the perfect position. As shown in Fig. 8(b), as the loading increased, more particles deviated from their original perfect position. These deviated particles increased the interaction with their neighboring causing the lattice re-arrangement [43]. This particle arrangement basically has a vital role to create small defects, which is indicated by changing particle stress color from light green to other colors (blue and red), mostly particles at loading points and center of the cell. Here, the force due to the compression is gradually localized into two chains with the formed symmetrical region, resulting in the agglomeration of deformation due to particles having the highest stress. In Figure 8(c), further loading leads to the highest stress distribution at the loading point initially, and reconstruction of the geometry of the chain propagated towards the loading direction and accumulate at the center of the cell. Thus, it initiates the bond-breaking simultaneously at the loading point and along the chain propagates vertically in the direction of loading. This bond-breaking leads to the small destruction of small clustering deformation in the center of the particle. With agglomerate deformation, the degree of force and stress increased at the center. Then, subsequent breaking bonds leading to the formation of initiated crack, which grows along the y-direction. The crack was initiated at the center of the cell, indicated by the highest stress (red-colored) where the established bonds are still in an unstable bonding, propagated in y-direction toward its loading platens. In the end, with the further increases in the applied loading, the region having the highest stress experienced more bond breaking, resulting in successive de-bonding along the y-direction. Then, it causes damaging the bond connection and ends up with the fracture of the system. After the bond breaking, the highest stress changes to the lower stress. This compressive loading induced alternating local and the whole binding configurations and its subsequent impact on the initiation of failure of the system. As a result, it breaks the polymer chain until complete rupture (See Fig. 8(d)).

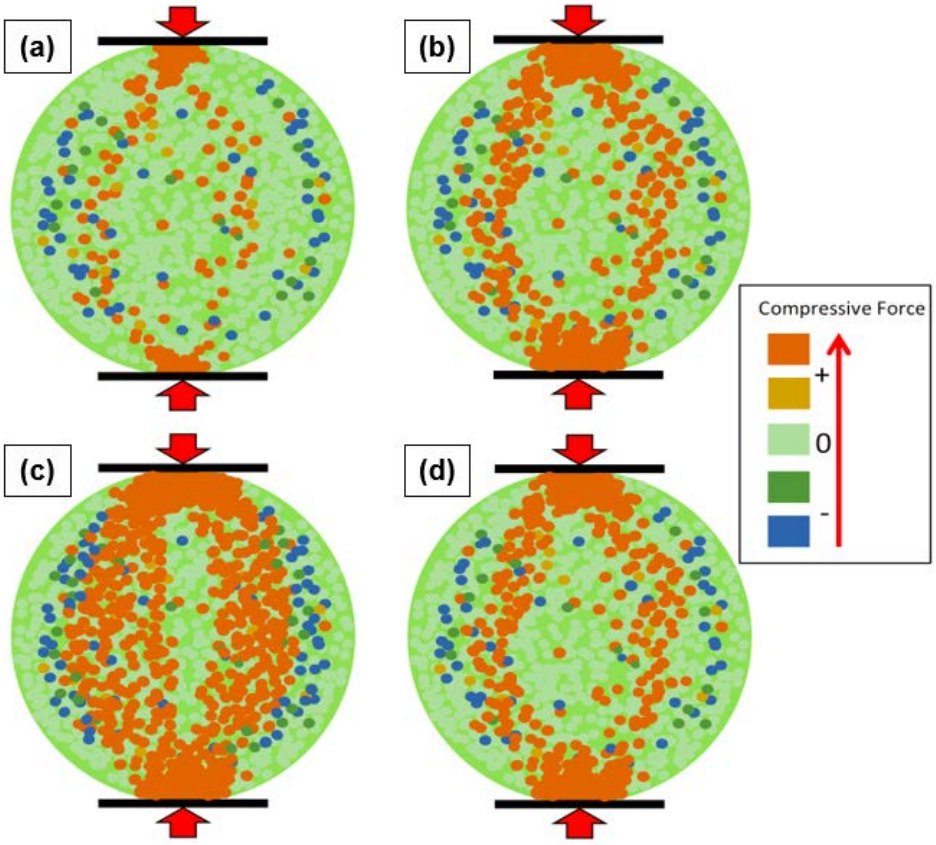

Fig. 8. The model of particle stress distribution in the bioplastic during the loading. Particles are colored cording to the corresponding particle stresses. Light green represents a perfect structure, blue or green showing for low stress, and red color for high stress. The system to be investigated is represented by a visualization cell, in which all particles are enclosed and interacted. The top and bottom surface is subjected to a compression force in y-direction

Table 6 shows a 2-dimensional model of the crack propagation path of the sample under the compression load. When a load is applied to the material, the cracks will propagate to a region with less bonding energy in the particle structure. As the region with lower interfacial energy, the interface between particles plays an important role in the crack propagation mechanism. When there are two types of particles (i.e. Particles A and B), the packing particles depend on the initial sizes of particles A and B. The red arrow is the position of the crack due to the applied load during the compression test, and the red line is the crack path in the sample.

As illustrated in Table 6, the surface area to volume ratio increases for material with smaller particle size. It introduces a larger proportion of particles to be found in the material. Those small particles induce small volume voids inside the material that makes the material to be more compact and stronger. The small volume voids prevent the crack propagation movement in the material. Under the applied load, the material with larger particles is likely to experience a severe disturbance of opening matrix angle that eventually results in bigger cracking compared to material with smaller particles. Larger particles also result in a material with larger voids inside it, allowing the crack easily propagate in the material since the material is less rigid.

Table 6. Illustration cracking progression

Type	Model	Crack Model
2 particles with different sizes + Particle A Particle B	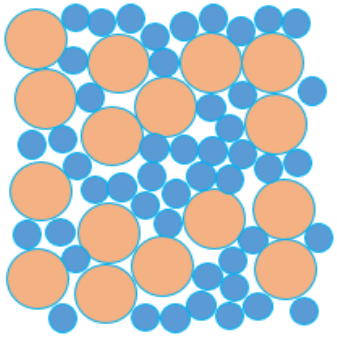	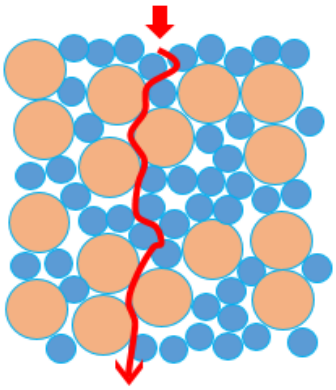
2 particles with almost the same sizes + Particle A Particle B	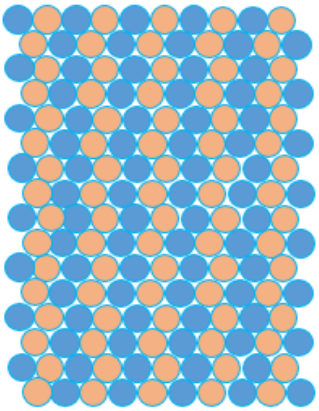	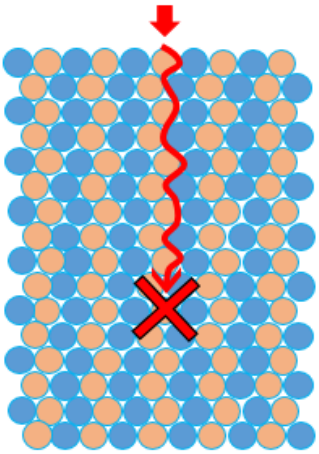

5. Conclusion

The mechanical and biodegradation properties of bioplastics from turmeric with various sizes were evaluated. The results showed that particle size affects the mechanical properties of the material. Turmeric particles with a small size tend to have a larger surface area, allowing for a stronger bonding area between particulates, and resulting in a higher stiffness and strength of the material. In contrast, larger particles have a lower interfacial strength, which makes a crack easier to propagate even at lower loads. However, there is a nonlinear trend found in this study where up to 250 µm has a higher strength than that of 125 µm. This is probably due to the non-uniform distribution of particles, which affects the strength of the material. Bioplastic biodegradability is also influenced by particle size. The smaller the size of the turmeric, the greater solubility it will be. Apart from the solubility parameters, a larger weight loss is also observed in a sample with smaller size, indicating good biodegradation.

Acknowledgements. *This study acknowledged RISTEK BRIN for Grant-in-aid Penelitian Terapan Unggulan Perguruan Tinggi (PTUPT) and Faculty of Engineering and Technology, Sampoerna University for the mechanical testing facilities.*

References

[1] Santana RF, Bonomo RCF, Gandolfi ORR, Rodrigues LB, Santos LS, dos Santos Pires AC, de Oliveira CP, Fontan RdCI, Veloso CM. Characterization of starch-based bioplastics

from jackfruit seed plasticized with glycerol. *Journal of Food Science and Technology*. 2018;55(1): 278-286.
[2] Sagnelli D, Hooshmand K, Kemmer GC, Kirkensgaard JJK, Mortensen K, Giosafatto CVL, Holse M, Hebelstrup KH, Bao J, Stelte W. Cross-linked amylose bio-plastic: A transgenic-based compostable plastic alternative. *International Journal of Molecular Sciences*. 2017;18(10): 2075.
[3] Salahin N, Begum RA, Hossian S, Ullah MM, Alam MK. Degradation of soil properties under ginger, turmeric, aroid, and jhum rice cultivation in hilly areas of Bangladesh. *Bangladesh Journal of Agricultural Research*. 2013;38(2): 363-371.
[4] Baek CS, Cho KH, Ahn JW. Effect of Grain Size and Replacement Ratio on the Plastic Properties of Precipitated Calcium Carbonate Using Limestone as Raw Material. *Journal of the Korean Ceramic Society*. 2014;51(2): 127-131.
[5] Codou A, Misra M, Mohanty AK. Sustainable biocarbon reinforced nylon 6/polypropylene compatibilized blends: Effect of particle size and morphology on performance of the biocomposites. *Composites Part A: Applied Science and Manufacturing*. 2018;112: 1-10.
[6] Farley R, Valentin FHH. Effect of particle size upon the strength of powders. *Powder Technology*. 1968;1(6): 344-354.
[7] Abdullah AHD, Pudjiraharti S, Karina M, Putri OD, Fauziyyah RH. Fabrication and characterization of sweet potato starch-based bioplastics plasticized with glycerol. *Journal of Biological Science*. 2019;19(1): 57-64.
[8] Lubis M, Harahap MB, Ginting MHS, Maysarah S, Gana A. The effect of ethylene glycol as plasticizer against mechanical properties of bioplastic originated from jackfruit seed starch and cocoa pod husk. *Nusantara Bioscience*. 2018;10(2): 76-80.
[9] Sumarni W, Prasetya AT, Rahayu EF. Effect of glycerol on physical properties of biofilms gembili starch (dioscorea esculenta)-chitosan. *Proceeding of Chemistry Conference*. 2017;2: 56-65.
[10] Oleyaei SA, Almasi H, Ghanbarzadeh B, Moayedi AA. Synergistic reinforcing effect of TiO_2 and montmorillonite on potato starch nanocomposite films: Thermal, mechanical and barrier properties. *CarbohydratePolymers*. 2016;152: 253-262.
[11] Borchani KE, Carrot C, Jaziri M. Biocomposites of Alfa fibers dispersed in the Mater-Bi® type bioplastic: Morphology, mechanical and thermal properties. *Composites Part A: Applied Science and Manufacturing*. 2015;78: 371-379.
[12] Vadori R, Mohanty AK, Misra M. The effect of mold temperature on the performance of injection molded poly (lactic acid)-based bioplastic. *Macromolecular Materials and Engineering*. 2013;298(9): 981-990.
[13] Nandiyanto ABD, Fiandini M, Ragadhita R, Sukmafitri A, Salam H, Triawan F. Mechanical and biodegradation properties of cornstarch-based bioplastic material. *Materials Physics and Mechanics*. 2020;44(3): 380-391.
[14] Triawan F, Nandiyanto ABD, Suryani IO, Fiandini M, Budiman BA. The influence of turmeric microparticles amount on the mechanical and biodegradation properties of cornstarch-based bioplastic material: From bioplastic literature review to experiments. *Materials Physics and Mechanics*. 2020;46(1): 99-114.
[15] Nandiyanto ABD, Andika R, Aziz M, Riza LS. Working volume and milling time on the product size/morphology, product yield, and electricity consumption in the ball-milling process of organic material. *Indonesian Journal of Science and Technology*. 2018;3(2): 82-94.
[16] Triawan F, Nakagawa R, Inaba K, Budiman BA, Kishimoto K. Experimental investigation of shear stress effect on the flexural behavior of aluminum foam beam. *Journal of Mechanical Science and Technology*. 2020;34: 1831-1836.

[17] Yunus M, Fauzan R. Effect of clove essential oil addition on characteristics of cassava starch bioplastic film incorporated zinc oxide-organoclay as reinforcement. *IOP Conference Series: Materials Science and Engineering*. 2019;536(1): 012138.
[18] Abdullah AHD, Fikriyyah AK, Dewantoro R. Fabrication and characterization of starch based bioplastics with palm oil addition. *Jurnal Sains Materi Indonesia*. 2019;20(3): 126.
[19] Kaisangsri N, Kerdchoechuen O, Laohakunjit N. Biodegradable foam tray from cassava starch blended with natural fiber and chitosan. *Industrial Crops and Products*. 2012;37(1): 542-546.
[20] Dos Santos Caetano K, Lopes NA, Costa TMH, Brandelli A, Rodrigues E, Flôres SH, Cladera-Olivera F. Characterization of active biodegradable films based on cassava starch and natural compounds. *Food Packaging and Shelf Life*. 2018;16: 138-147.
[21] Luchese CL, Spada JC, Tessaro IC. Starch content affects physicochemical properties of corn and cassava starch-based films. *Industrial Crops and Products*. 2017;109: 619-626.
[22] Petnamsin C, Termvejsayanon N, Sriroth K. Effect of particle size on physical properties and biodegradability of cassava starch/polymer blend. *Agriculture and Natural Resources*. 2000;34(2): 254-261.
[23] Dai L, Qiu C, Xiong L, Sun Q. Characterisation of corn starch-based films reinforced with taro starch nanoparticles. *Food Chemistry*. 2015;174: 82-88.
[24] Ibrahim H, Farag M, Megahed H, Mehanny S. Characteristics of starch-based biodegradable composites reinforced with date palm and flax fibers. *Carbohydrate Polymers*. 2014;101: 11-19.
[25] Ibrahim MIJ, Sapuan SM, Zainudin ES, Zuhri MYM. Potential of using multiscale corn husk fiber as reinforcing filler in cornstarch-based biocomposites. *International Journal of Biological Macromolecules*. 2019;139: 596-604.
[26] Silva-Guzmán JA, Anda RR, Fuentes-Talavera FJ, Manríquez-González R, Lomelí-Ramírez MG. Properties of thermoplastic corn starch based green composites reinforced with barley (Hordeum vulgare L.) straw particles obtained by thermal compression. *Fibers and Polymers*. 2018;19(9): 1970-1979.
[27] Campos A, Marconcini JM, Imam SH, Klamczynski A, Ortis WJ, Wood DH, Williams TG, Martins-Franchetti SM, Mattoso LHC. Morphological, mechanical properties and biodegradability of biocomposite thermoplastic starch and polycaprolactone reinforced with sisal fibers. *Journal of Reinforced Plastics and Composites*. 2012;31(8): 573-581.
[28] Ilyas RA, Sapuan SM, Ishak MR, Zainudin ES. Water transport properties of bio-nanocomposites reinforced by sugar palm (Arenga Pinnata) nanofibrillated cellulose. *Journal of Advanced Research in Fluid Mechanics and Thermal Sciences*. 2018;51(2): 234-246.
[29] Shahrim NA, Rani NNSA, Sarifuddin N, Zaki HHM, Azhar AZA. Effects of banana skin powder on properties of jackfruit seed starch/poly (vinyl alcohol) PVA film. In: *Proc. of AMCT 2017*. 2017. p.571.
[30] Cinelli P, Chiellini E, Lawton JW, Imam SH. Foamed articles based on potato starch, corn fibers and poly (vinyl alcohol). *Polymer Degradation and Stability*. 2006;91(5): 1147-1155.
[31] Duanmu J, Gamstedt EK, Pranovich A, Rosling A. Studies on mechanical properties of wood fiber reinforced cross-linked starch composites made from enzymatically degraded allylglycidyl ether-modified starch. *Composites Part A: Applied Science and Manufacturing*. 2010;41(10): 1409-1418.
[32] Dash KK, Ali NA, Das D, Mohanta D. Thorough evaluation of sweet potato starch and lemon-waste pectin based-edible films with nano-titania inclusions for food packaging applications. *International Journal of Biological Macromolecules*. 2019;139: 449-458.

[33] Li X, Qiu C, Ji N, Sun C, Xiong L, Sun Q. Mechanical, barrier and morphological properties of starch nanocrystals-reinforced pea starch films. *Carbohydrate Polymers*. 2015;121: 155-162.
[34] Hemsri S, Grieco K, Asandei AD, Parnas RS. Wheat gluten composites reinforced with coconut fiber. *Composites Part A: Applied Science and Manufacturing*. 2012;43(7): 1160-1168.
[35] Wu Q, Rabu J, Goulin K, Sainlaud C, Chen F, Johansson E, Olsson RT, Hedenqvist MS. Flexible strength-improved and crack-resistant biocomposites based on plasticised wheat gluten reinforced with a flax-fibre-weave. *Composites Part A: Applied Science and Manufacturing*. 2017;94: 61-69.
[36] Yang W, Kenny JM, Puglia D. Structure and properties of biodegradable wheat gluten bionanocomposites containing lignin nanoparticles. *Industrial Crops and Products*. 2015;74: 348-356.
[37] Kiruthika AV, Priyadarzini TRK, Veluraja K. Preparation, properties and application of tamarind seed gum reinforced banana fibre composite materials. *Fibers and Polymers*. 2012;13(1): 51-56.
[38] Sultan NFK, Johari WLW. The development of banana peel/corn starch bioplastic film: A preliminary study. *Bioremediation Science and Technology Research*. 2017;5(1): 12-17.
[39] Agustin YE, Padmawijaya KS. Effect of glycerol and zinc oxide addition on antibacterial activity of biodegradable bioplastics from chitosan-kepok banana peel starch. *IOP Conference Series: Materials Science and Engineering*. 2017;223(1): 012046.
[40] Nandiyanto ABD, Oktiani R, Ragadhita R. How to read and interpret FTIR spectroscope of organic material. *Indonesian Journal of Science and Technology*. 2019;4(1): 97-118.
[41] Valdés A, Fenollar O, Beltrán A, Balart R, Fortunati E, Kenny JM, Garrigós MC. Characterization and enzymatic degradation study of poly (ε-caprolactone)-based biocomposites from almond agricultural by-products. *Polymer Degradation and Stability*. 2016;132: 181-190.
[42] Sukrawan Y, Hamdani A, Mardani SA. Effect of bamboo weight faction on mechanical properties in non-asbestos composite of motorcycle brake pad. *Materials Physics and Mechanics*. 2019;42(3): 367-372.
[43] Nandiyanto ABD, Triawan F, Firly R, Abdullah AG, Aono Y, Inaba K, Kishimoto K. Identification of micro-mechanical characteristics of monoclinic tungsten trioxide microparticles by nanoindentation technique. *Materials Physics and Mechanics*. 2019;42(3): 323-329.
[44] Wu J, Feng M, Chen Z, Mao X, Han G, Wang Y. Particle size distribution effects on the strength characteristic of cemented paste backfill. *Minerals*. 2018;8(8): 322.